Heat capacity and thermal expansion of the itinerant helimagnet MnSi

2008 J. Phys.: Condens. Matter 20 235222

(http://iopscience.iop.org/0953-8984/20/23/235222)

J. Phys.: Condens. Matter **20** (2008) 235222 (6pp) doi:10.1088/0953-8984/20/23/235222

Heat capacity and thermal expansion of the itinerant helimagnet MnSi

S M Stishov[1], A E Petrova[1], S Khasanov[2], G Kh Panova[3], A A Shikov[3], J C Lashley[4], D Wu[5] and T A Lograsso[5]

[1] Institute for High Pressure Physics, Troitsk, Moscow Region, Russia
[2] Institute of Solid State Physics, Chernogolovka, Moscow Region, Russia
[3] Russian Research Center, Kurchatov Institute, Moscow, Russia
[4] Los Alamos National Laboratory, Los Alamos, 87545 NM, USA
[5] Ames Laboratory, Iowa State University, Ames, IA 50011, USA

E-mail: sergei@hppi.troitsk.ru (S M Stishov)

Received 21 January 2008, in final form 13 March 2008
Published 6 May 2008
Online at stacks.iop.org/JPhysCM/20/235222

Abstract

The heat capacity and thermal expansion of a high quality single crystal of MnSi were measured at ambient pressure at zero and high magnetic fields. The calculated magnetic entropy change in the temperature range 0–30 K is less than $0.1R$, a low value that emphasizes the itinerant nature of magnetism in MnSi. A linear temperature term dominates the thermal expansion coefficient in the range 30–150 K, which correlates with an enhancement of the linear electronic term in the heat capacity. A surprising similarity among the variations of the heat capacity, thermal expansion coefficient and temperature derivative of the resistivity is observed through the phase transition in MnSi. Specific forms of the heat capacity, thermal expansion coefficient and temperature derivative of resistivity at the phase transition to a helical magnetic state near 29 K are interpreted as the combination of sharp first-order features and broad peaks or shallow valleys of as yet unknown origin. The appearance of these broad satellites probably hints at a frustrated magnetic state slightly above the transition temperature in MnSi.

(Some figures in this article are in colour only in the electronic version)

1. Introduction

Extensive studies of the physical properties of the itinerant helimagnet MnSi have been carried out for decades and have brought up a number of intriguing results of general physical significance. Magnetic ordering of an unknown nature in MnSi, occurring around 30 K, was reported for the first time in [1]. The magnetic moment per atom Mn at low temperature was found to equal 0.4 μ_B; whereas, fitting susceptibility data to a Curie–Weiss law gave an effective moment of 2.2 μ_B per Mn in the paramagnetic phase [2]. This difference is usually considered as a signature of the itinerant nature of magnetism.

The crystal structure of MnSi as well as some other silicides and germanides (FeSi, CoSi, FeGe, etc) of the transition metals belongs to the B 20 type, cubic space group (T^4) [3]. The space group $P2_13$ does not contain a center of symmetry and allows a non-zero value of the Dzyaloshinski–Moria term in energy $D[S_i \times S_j]$, arising as a result of small relativistic spin–lattice and spin–spin interactions [4, 5]. This term, though being small, could cause a long wave modulation of magnetic spin structure. Consistent with theory, magnetic order in MnSi was identified as a long period ferromagnetic spiral or helical spin structure [6]. At zero magnetic field, the wavevector q of the helix is directed along a space diagonal of the cubic unit cell of MnSi, so spins are ferromagnetically aligned in layers parallel to the (111) plane. The magnetic moment of each consecutive layer is turned by a small angle with respect to a previous one, therefore forming a spiral with a pitch of 180 Å ($q = 0.035$ Å^{-1}). The wavevector can be aligned in different directions on application of a magnetic field of about ≈0.2 T. At a magnetic field of ≈0.6 T, a field-induced ferromagnetic structure appears [2]. So the magnetic properties of MnSi are governed by a hierarchy of three energy scales that are: the exchange interaction, defining in-plane ferromagnetic ordering, the weak Dzyaloshinski–Moria spin–orbit interaction, producing chirality of the spin structure and a weaker anisotropic exchange-crystal anisotropy terms directing the wavevector q along the space diagonal of the cubic cell.

An order parameter in MnSi has two components, characterizing the spin and chiral orders and can be described by a complex vector $S = S_0 e^{iqz}$. A Landau expansion of the free energy in powers of the order parameter does not contain the odd terms due to time-reversal symmetry. This suggests a second-order nature of the phase transition in MnSi, though fluctuations and interaction of the magnetic order parameter with other degrees of freedom could transform the phase transition into first order [7–9, 12]. Bak and Jensen [9], predicted a first-order transition in MnSi and claimed experimental support for it [10]. We also note that the phase transition into the helical state in FeGe, which is a structural and magnetic analog of MnSi, is first order [11].

Another complication specific for to chiral spin systems is the coupling of spin and chiral order. If they were not coupled (see for instance [13, 14]), one could expect two phase transitions in substances, like MnSi, first to the spin ordered state, then to the chiral state. However, despite theoretical conclusions and speculations, all physical properties of MnSi studied until very recently seemed to be continuous across the phase-transition line at ambient pressure. Yet, the seemingly successful attempt of measuring some critical indexes at the phase transition in MnSi hinted at a chiral universality class [15]. Recently, strong evidence was obtained for a first-order phase transition in MnSi at ambient pressure [16] (see in this connection also [11]). pressure [16] (see in this connection also [11]). Nevertheless, some other remarkable properties of MnSi and its phase transition are not still understood. Quantities, like thermal expansion coefficient [18, 16], heat capacity [19, 16], and temperature coefficient of resistivity [17, 16] display a well-defined round maximum of enigmatical origin on the high temperature side of their corresponding peaks at the phase transition. To shed light on these problems, heat capacity and thermal expansion in magnetic fields are reported for a high quality MnSi single crystal at ambient pressure.

2. Sample preparation and its characteristics

The intermetallic compound MnSi melts congruently and single crystals of good quality can be grown by direct crystallization from a melt. The single crystal of MnSi used in the current study was grown in a resistance furnace by the Bridgman technique[6]. Appropriate quantities of manganese (99.99% pure) and silicon (99.999% pure) were cleaned and arc melted several times under an argon atmosphere. The alloy was then cast into a copper-chilled mold to ensure compositional homogeneity throughout the ingot. The as-cast ingot was sealed in a quartz tube and heated under vacuum to 1100 °C. After reaching 1100 °C, the growth chamber was backfilled with ultra high purity argon to a pressure of 1.03×10^5 Pa. Following pressurization, heating was continued until the ingot reached a temperature of 1360 °C and held there for one hour before being withdrawn from the furnace at a rate of 5 mm h^{-1}. The ingot broke into several pieces after extraction from the quartz tube. The largest piece (20 mm in diameter and 40 mm height) was examined by x-ray Laue back-reflection and appeared to be a single crystal. Samples of necessary size and orientation for various experiments were cut by low-power spark erosion.

Structural perfection of the MnSi single crystal was studied by means of a two-crystal x-ray spectrometer. Rocking curve data were collected in the Θ—mode using the (110) MnSi reflection and Cu Kα_1 radiation selected with a *Si*(400) monochromator. Overall mosaicity of the sample appeared to be less than 0.1°. The lattice constant of MnSi was measured with a Siemens D-500 x-ray diffractometer using Cu Kα-radiation and the (440) reflection of the crystal in a Θ–2Θ scanning mode. The measured doublet peak (K$\alpha_{1,2}$) was fitted using SPLIT PEARSON functions. For a lattice parameter of MnSi at 298 K, we obtained $a = 4.5598(2)$ Å, compared to previous reports of 4.5603(2) Å [20] and 4.559(1) Å [21].

Elastic moduli of MnSi, measured by a pulse ultrasound technique, are: $c_{11} = 283.30 \pm 1.62$ GPa, $c_{12} = 64.06 \pm 1.92$ GPa, $c_{44} = 117.86 \pm 0.52$ GPa, and bulk modulus $K = 1/3(c_{11} + 2c_{12}) = 137.14$ GPa [22]. The Debye temperature of MnSi, calculated from values of the elastic constants, is $\Theta_D \approx 500$ K. These values generally agree with earlier determinations [23].

3. Experimental technique

Heat capacity was measured with an adiabatic vacuum calorimeter using a heat pulse method. Overall accuracy of heat capacity measurements was about 1–1.5%. Linear thermal expansion measurements were performed in a capacitance dilatometer with a resolution of about 0.05 Å (for an extensive description of the technique, see [24]). In all these experiments, temperature was measured by calibrated Cernox thermometers with overall resolution and accuracy not worse than 0.05 K. The heat capacity and thermal expansion measurements in magnetic fields were performed by making use of superconducting solenoids.

4. Heat capacity

The heat capacity of MnSi divided by temperature in the temperature range 2–40 K is shown in figure 1. As is seen more clearly in figure 2 a sharp peak in C_p at ∼28.8 K, appears as a slightly broadened delta function on top of a rounded maximum. This feature of the transition is transformed into a sharp dip at the bottom of shallow minimum in case of the thermal expansion coefficient, which will be discussed later (see also [16]). Two more curves in figure 1 reflect the influence of a magnetic field on the heat capacity of MnSi. As is known, a magnetic field of about 0.6 T at low temperature aligns spins in MnSi along the direction of the applied field, therefore creating a field-induced ferromagnetic state [2]. Consequently, a magnetic field of certain magnitude will completely destroy the phase transition in MnSi, as illustrated in figures 1 and 2. On the other hand, moderate magnetic fields, as pointed out with respect to the thermal expansion coefficient [16], have little effect on the heat capacity of the helical phase even at temperatures close to T_c. The latter is not

[6] Materials Preparation Center, Ames Laboratory, US-DOE, Ames, IA, USA.

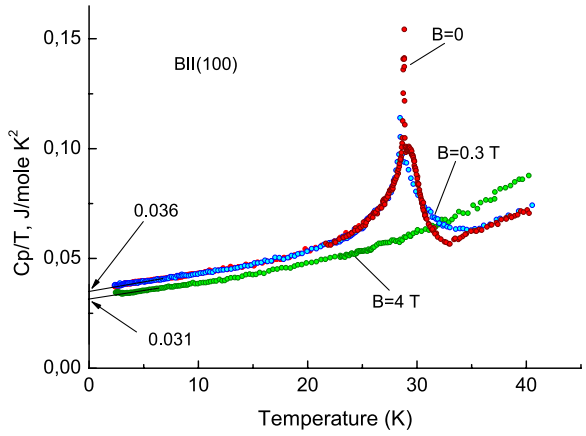

Figure 1. Temperature dependence of heat capacity divided by temperature in MnSi. Short extrapolations give values for the linear terms in the heat capacity $\gamma = 36$ mJ mol^{-1} K^{-2} ($B = 0$) and $\gamma = 31$ mJ mol^{-1} K^{-2} ($B = 4$ T).

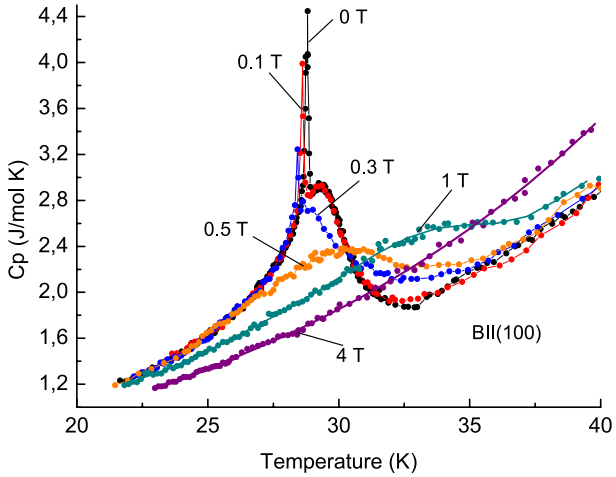

Figure 2. Temperature dependence of heat capacity near the phase transition in MnSi. It is seen that magnetic fields up to 0.3 T practically do not affect the heat capacity of the helical phase.

true for the paramagnetic phase whose heat capacity readily responds to modest magnetic fields at temperatures close to and slightly above T_c.

Now we turn to low temperature behavior of C_p/T. The standard way of analyzing heat capacity, by plotting data C_p/T versus T^2, does not work in the present case because of a small phonon contribution (see figure 3). However, a T-linear coefficient of the heat capacity of MnSi is easily obtained by a short graphic extrapolation of the low temperature curves of C_p/T to zero temperature as illustrated in figure 1. The results yield $\gamma = 36$ mJ mol^{-1} K^{-2} ($B = 0$) and 31 mJ mol^{-1} K^{-2} ($B = 4$ T). The magnitude of γ for $B = 0$ is in good agreement with an earlier estimate, corrected for an obvious error [25]. Though the electron mass enhancement in MnSi is obvious from the high value of γ, the ratio m^*/m is unknown due to uncertainty in the electron concentration in MnSi. A calculated value of γ_0 for the case of two free electrons per molecule of MnSi is $\gamma_0 = 1.0$ mJ mol^{-1} K^{-2}, leading to the mass ratio in MnSi of $m^*/m \approx 36$.

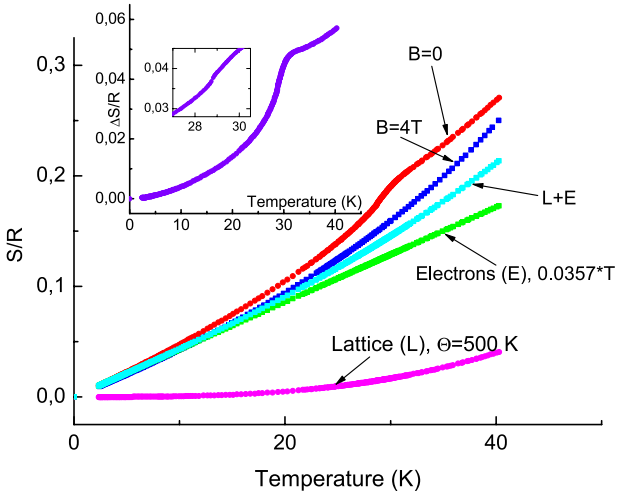

Figure 3. Entropy of MnSi calculated from the heat capacity (R—gas constant). The electron contribution is taken in the conventional form as γT. A Debye model with $\Theta_D = 500$ K was used to estimate the lattice contribution to entropy. The difference between total entropy and electron and phonon contributions $\Delta S = S - S_{el} - S_{ph}$ is shown in the inset. A tiny entropy jump at the phase transition is illustrated in the smaller inset.

Figure 3 gives plot of entropy S and its constituents in MnSi as a function of temperature. As seen, an electronic contribution makes up a dominant fraction of the total entropy due to the relatively large electron effective mass m^* (we neglect here a possibility of changing of m^* with temperature). At the same time, the calculated phonon contribution is rather small in the temperature range under study. The difference between total entropy and the sum of electronic and phonon contributions, which characterizes the magnetic or spin ordering in MnSi, is less than $0.1R$ (see inset in figure 3) and once again identifies the itinerant nature of magnetism in MnSi.

5. Thermal expansion

The temperature variation of the linear thermal expansion coefficient $\beta = (1/L_0)(dL/dT)$ of MnSi is shown in figure 4. In the temperature range 0–35 K, the behavior of β is defined by magneto-volume and fluctuation effects arising as a result of magnetic moments ordering. Plotting the data as β/T versus T^2 does not reveal any noticeable lattice contribution but exposes a remarkable linear in temperature increase in β over the temperature range 35–150 K (see the inset in figure 4), which correlates with the enhanced electronic linear temperature term in the heat capacity. In figure 5, the thermal expansion $\Delta L/L_0$ ($L_0 = L_{301\,K}$) of MnSi, calculated by integration of the dilatometric data, is compared with powder neutron diffraction and single crystal x-ray data [26]. All the data agree within 0.02%. The x-ray data set the absolute length scale, though they do not demonstrate enough resolution to permit seeing subtle features of the phase transition that dilatometric measurements do. Figure 6 illustrates the influence of magnetic field on the thermal expansion coefficient of MnSi. In the case of helical spin ordering, a magnetic field is not directly

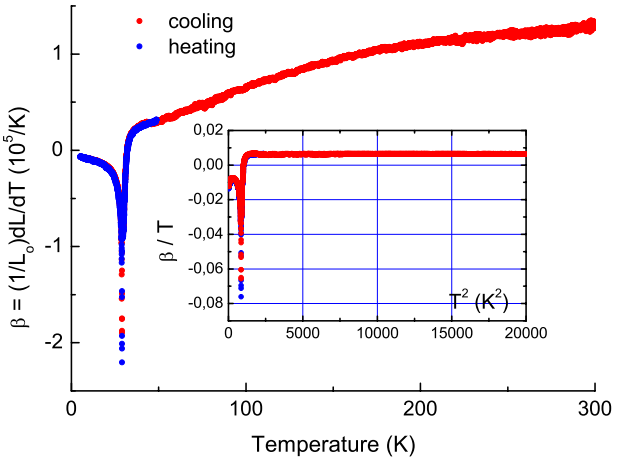

Figure 4. Linear thermal expansion coefficient of MnSi (β). As was mentioned in [16], the thermodynamic hysteresis at the phase transition is expected to be about 0.005 K and could hardly be observed. It is seen in the inset that a linear term dominates behavior of β in the range 30–150 K.

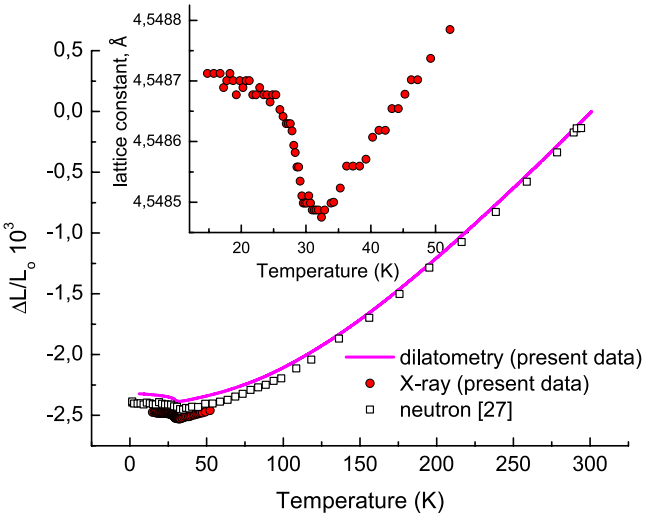

Figure 5. Linear thermal expansion of MnSi.

coupled with the order parameter, and hence, no significant effect of magnetic field on the phase transition is expected until the field-induced ferromagnetic state appears at about 0.35 T [27]. Fast degradation of sharp features of the transition for fields between 0.3 and 0.4 T clearly indicates formation of a ferromagnetic spin structure in MnSi. The same situation was also seen in the heat capacity response to moderate magnetic fields (figures 1, 2). A magnetic phase diagram, given in figure 7, summarizes the influence of a magnetic field on the phase transition and other specific features in the thermal expansion and heat capacity of MnSi.

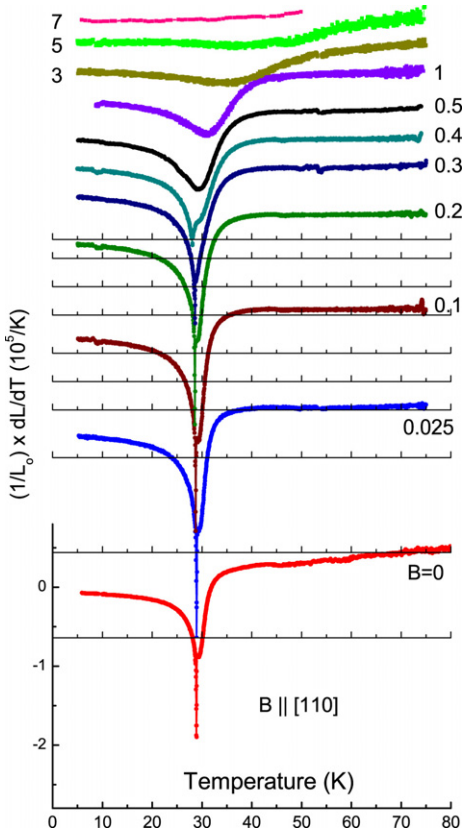

Figure 6. Linear thermal expansion coefficient of MnSi in magnetic fields. Values of magnetic fields are given in tesla.

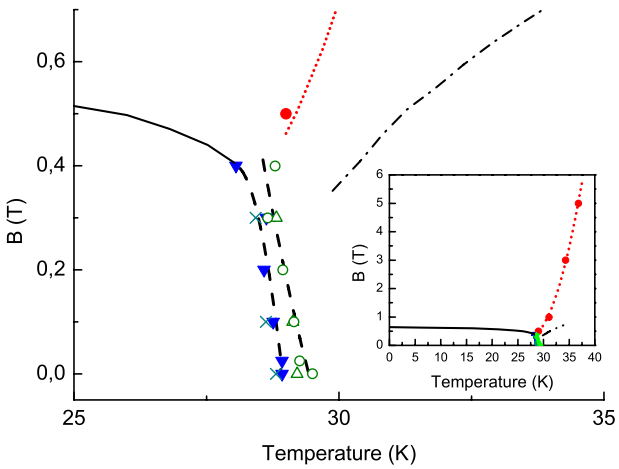

Figure 7. Magnetic phase diagram of MnSi. Solid triangles and crosses are coordinates of the phase transition from thermal expansion and heat capacity experiments, respectively. Open circles and triangles record the broad minima and maxima of the thermal expansion coefficients and heat capacity. A solid line is drawn in accordance with data [10]. Close circles mark the minima of thermal expansion coefficients above 0.4 T. Broken and dotted lines are guides for eyes.

6. Discussion

Almost perfect similarity between the heat capacity, the linear thermal expansion coefficient and the temperature derivative of resistivity in the phase-transition region of MnSi is displayed in figure 8. As is seen from figure 8, a sharp peak on the low temperature side of a rounded maximum or correspondingly a sharp dip to the left of the bottom of a rounded minimum in heat capacity, thermal expansion

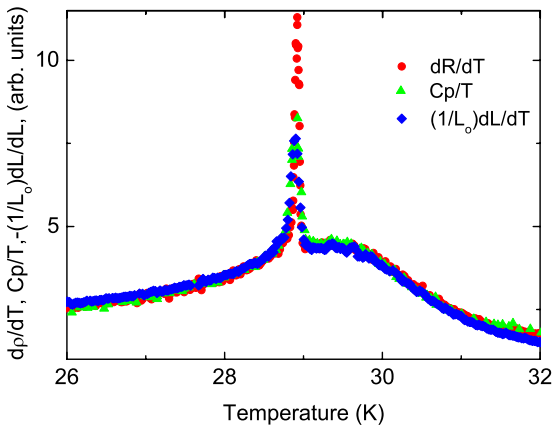

Figure 8. Unified temperature dependence of the heat capacity, the temperature derivative of resistivity and the linear thermal expansion coefficient of MnSi in the phase-transition region. All curves were reduced by a linear transformation. Note that data for the thermal expansion coefficient were taken with the inverse sign.

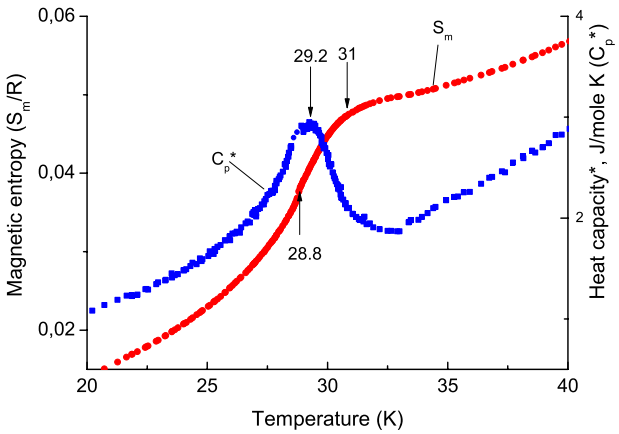

Figure 9. Magnetic part of entropy $S_{\rm m}/R$ (left ordinate) and heat capacity C_p (right ordinate) of MnSi in the vicinity of its phase transition. The peak in C_p was eliminated for a better view of the rounded maximum.

coefficient and temperature derivatives of resistivity is an intrinsic property of the phase transition in the itinerant helical magnet state of MnSi. The sharp peaks most likely identify the phase transition in MnSi as weakly first order. This conclusion is certainly supported by the well forgotten result of [10] (see also figure 7), where a finite value was found for the critical magnetic field that corresponds to a transition from conical to ferromagnetic spin structure at the phase-transition temperature. It also needs to be mentioned here that, as was explicitly shown in [28], the second-order phase transition in the itinerant weak ferromagnet $ZrZn_2$ displayed typical mean field behavior with simple jumps in C_p and $d\rho/dT$ at the phase-transition point that is drastically different from what we see in MnSi. This clearly supports our interpretation of the nature of the phase transition in MnSi. However, above considerations leave unattended a question on nature of the rounded maximum demonstrated in figure 8. Certain insight comes from the behavior of magnetic entropy and the heat capacity shown in figure 9 where the peak in C_p was removed for clarity.

As seen from the entropy curve, some ordering process starts around 31 K, reaches its culmination at the temperature corresponding to the top of the round maximum of C_p (29.2 K), and is interrupted by the first-order phase transition a half of a degree below (28.8 K). The overall behavior of the entropy and the heat capacity looks like the system is preparing to take some sort of frustrated magnetic configuration but then some subtle interaction comes into play and the system collapses into the helical phase. We are not in a position to discuss the character of this interaction here, but perhaps a fourth energy scale is needed to unlock the configuration space, therefore facilitating the phase transition in MnSi (striction effects also might be relevant to this case [12]).

7. Conclusion

We have measured the heat capacity and thermal expansion of a high quality single crystal of MnSi at ambient pressure for zero and high magnetic fields. Specific forms of the heat capacity and the thermal expansion coefficient in the vicinity of the magnetic phase transition (sharp peak/dip at the top or bottom of a continuous anomaly) do not change much with magnetic field until a field-induced ferromagnetic structure is formed at about 0.35–0.4 T. Note that a finite value of magnetic field needed for forming the ferromagnetic structure of MnSi at the transition temperature signifies the first-order nature of the phase transition (see in this connection [9]). An electronic contribution constitutes a major part of the total entropy of MnSi at the transition temperature. Spin ordering entropy appears to be less than $0.1R$, therefore emphasizing the itinerant nature of magnetism in MnSi. Universal behavior of the thermodynamic and transport properties of MnSi in the phase-transition region was discovered, which indicate spin fluctuations as a primary factor defining specific features of the mentioned quantities at the phase transition. The puzzling rounded maxima or minima observed in thermodynamic and transport properties on the high temperature side of the corresponding peaks at the phase-transition point are tentatively interpreted as a consequence of a spin frustrated state of MnSi that is destroyed by the transition into a helical state.

Acknowledgments

Authors are grateful to V A Sidorov and V V Krasnorussky for technical assistance. DW and TAL wish to acknowledge the support of the US Department of Energy, Basic Energy Sciences. SMS and AEP appreciate support of the Russian Foundation for Basic Research (grant 06-02-16590), Program of the Physics Department of RAS on Strongly Correlated Systems and Program of the Presidium of RAS on Physics of Strongly Compressed Matter. Work at Los Alamos was performed under the auspices of the US Department of Energy, Office of Science.

References

[1] Williams H J, Wernick J H, Sherwood R C and Wertheim G K 1966 *J. Appl. Phys.* **37** 1256
[2] Wernick J H, Wertheim G K and Sherwood R C 1972 *Mater. Res. Bull.* **7** 1431
[3] Borén B 1933 *Ark. Kemi Min. Geol.* **11A** 1
[4] Dzyaloshinski I 1958 *J. Phys. Chem. Solids* **4** 241
[5] Moriya T 1960 *Phys. Rev.* **120** 91
[6] Ishikawa Y, Tajima K, Bloch D and Roth M 1976 *Solid State Commun.* **19** 525
[7] Brazovskii S A, Dzyaloshinski I E and Kukharenko B G 1976 *Zh. Eksp. Teor. Phys.* **70** 2257
Brazovskii S A, Dzyaloshinski I E and Kukharenko B G 1976 *Sov. Phys.—JETP* **43** 1178 (Engl. Transl.)
[8] Dzyaloshinski I E 1977 *Zh. Eksp. Teor. Phys.* **72** 1930
Dzyaloshinski I E 1977 *Sov. Phys.—JETP* **45** 1014 (Engl. Transl.)
[9] Bak P and Jensen M H 1980 *J. Phys. C: Solid State Phys.* **13** L 881
[10] Ishikawa Y, Komatsubara T and Bloch D 1977 *Physica* B **86–88** 401
[11] Pedrazzini P, Wilheim H, Jaccard D, Jarlborg T, Schmidt M, Hanfland M, Akselrud L, Yuan H Q, Schawarz U, Grin Yu and Steglish F 2007 *Phys. Rev. Lett.* **98** 047204
[12] Larkin A I and Pikin S A 1969 *Sov. Phys.—JETP-USSR* **29** 891
[13] Diep H T 1989 *Phys. Rev.* B **39** 397
[14] Plumer M L and Mailhot A 1994 *Phys. Rev.* B **50** 16113
[15] Grigoriev S V, Maleyev S V, Okorokov A I, Chetverikov Yu O, Georgii R, Böni P, Lamago D, Eckerlebe H and Pranzas K 2005 *Phys. Rev.* B **72** 134420
[16] Stishov S M, Petrova A E, Khasanov S, Panova G Kh, Shikov A A, Lashley J C, Wu D and Lograsso T A 2007 *Phys. Rev.* B **76** 052405
[17] Petrova A E, Bauer E D, Krasnorussky V and Stishov S M 2006 *Phys. Rev.* B **74** 092401
[18] Matsunaga M, Ishikawa Y and Nakajima T 1982 *J. Phys. Soc. Japan* **51** 1153
[19] Lamago D, Georgii R, Pfleiderer C and Böni P 2006 *Physica* B **385/386** 385
[20] Jorgensen J E and Rasmussen S 1991 *Powder Diffract.* **6** 194
[21] Okada S, Shishido T, Ishizawa Y, Ogawa M, Kudou K, Fukuda T and Lundström T 2001 *J. Alloys Compounds* **317/318** 315
[22] Gromnitskaya E L 2007 Institute for High Pressure Physics, Troitsk, unpublished
[23] Zinoveva G P, Andreeva L P and Geld P V 1974 *Phys. Status Solidi* **23** 711
[24] Schmiedeshoff G M, Lounsbury A W, Luna D J, Tracy S J, Schramm A J, Tozer S W, Correa V F, Hannahs S T, Murphy T P, Palm E C, Lacerda A H, Bud'ko S L, Canfield P C, Smith J L, Lashley J C and Cooley J C 2006 *Rev. Sci. Instrum.* **77** 123907
[25] Fawcett E, Maita J P and Wernick J H 1970 *Int. J. Magn.* **1** 29
[26] Fåk B, Sadykov R A, Flouquet J and Lapertot G 2005 *J. Phys.: Condens. Matter* **17** 1635
Sadykov R A 2007 private communication
[27] Grigoriev S V, Maleyev S V, Okorokov A I, Chetverikov Yu O and Eckerlebe H 2006 *Phys. Rev.* B **73** 224440
[28] Yelland E A, Yates S J C, Taylor O, Griffiths A, Hayden S M and Carrington A 2005 *Phys. Rev.* B **72** 184436